

Abyssal flow in a two-layer model with sloping boundaries and a mid-ocean ridge

Helén C. Andersson

1 Introduction

The vast abyssal ocean is comprised of layers of very cold and dense water. As this is true even for the deep water of the tropics, the source of this water must be of polar origin. The vertical circulation that enables ventilation of these layers is driven by surface processes resulting from air-sea interaction. Heat loss of the surface water in combination with increased salinity due to evaporation or ice formation produces a dense water that sinks toward the ocean bottom. During the descent its density gets reduced due to entrainment of lighter water, and the final depth of the water mass is a function of surface density and the extent of mixing during the descent. The water then flows in a deep, large-scale circulation that fills the ocean basins. Lighter water rises to the surface and flows in surface currents to the polar regions to replace the water that has sunk.

The abyssal ocean can be divided into three layers: an intermediate layer from the base of the thermocline to about 1500 m, a deep layer below this and finally a bottom layer that is in contact with the sea floor. The sources of new abyssal waters are few as there is only a small number of regions that can produce surface water dense enough to sink to the deeper layers of the ocean. Intermediate waters form mainly in the Labrador Sea and the sub polar areas from extensive cooling but also in the Mediterranean due to high evaporation rates. Deep water formation occurs in the Nordic seas where cooling, in combination with salt release on the shelves due to ice formation, creates a dense water mass that spills in to the North Atlantic, mainly through the Faeroe Bank Channel. In the Southern Hemisphere deep and bottom water are formed at the Antarctic continent with the main location in the Weddell Sea.

Obtaining long-term measurements of the circulation in the deep ocean is difficult and our understanding of these flows is hence somewhat limited. Tracer studies have lately increased the knowledge of the flow and information is also gained from models. Stommel [1] developed a model where the abyssal circulation is a result of the sinking of deep water in high latitudes which is replaced by upwelling of deep water through the thermocline. With geographically constricted sources of deep water at the poles, the return flow is specified to be equally distributed over the entire interface between the two layers. The resulting interior geostrophic Sverdrup flow is always poleward, the vertically uniform flow of the abyss being the result of its single layer representation. The Sverdrup interior is independent of the position of the sources (see section 2) and vanishes at the equator. Western boundary

currents are added to the solution in order to satisfy mass balance and these currents are also the only possibility for a flow across the equator.

Stommel's [1] model shows the characteristics of the mean abyssal flow. However, strong baroclinic motion evident from observations are not captured by the model. Topographic features in the basin will also affect the flow. In the present study, the objective is to find an analytical solution for a model of flow in a closed basin with bottom topography and stratification. We first explore the solution to a homogeneous flow with sloping northern and western boundaries and a mid ocean ridge, before turning to the two-layer model.

2 The homogeneous model

We will first consider the case in which the ocean is represented by a single active layer. The bottom topography of the basin is shown in Fig. 1. The 500 km wide western and northern boundaries slope linearly from the ocean surface to the flat ocean floor at a depth of 4000 m. The mid-ocean ridge has a height of 3000 m and is 1000 km wide. The southern boundary is located at the equator. The isobaths of the basin geometry are shown in Fig. 2, where the slope region on the northern boundary is added for analytical convenience.

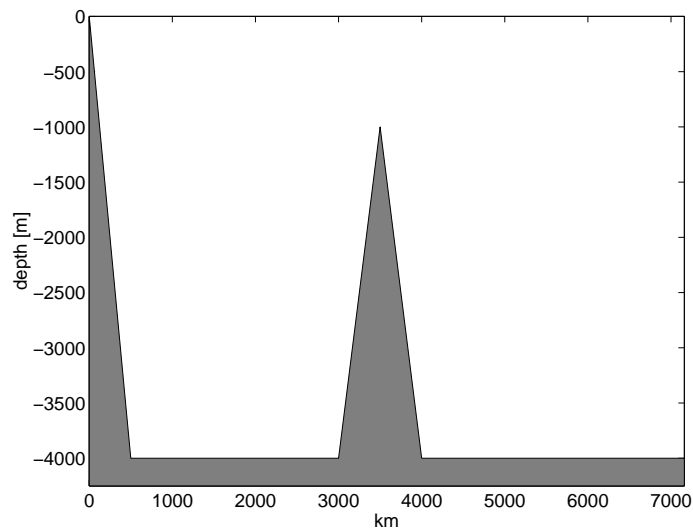


Figure 1: The bottom topography of the model basin.

The flow in the basin is driven by uniform upwelling, w_o , through the upper surface over the flat bottom (not over the boundaries). The layer gains water by sinking of upper layer water at the north-eastern corner. In the linear and steady state the interior flow is in geostrophic balance, hydrostatic and on a β -plane described by

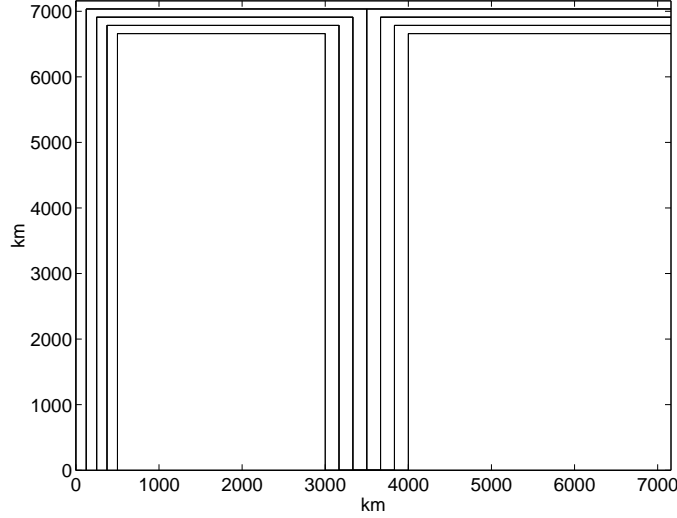


Figure 2: The isobaths of northern hemisphere model basin.

$$fv - g' \frac{\partial \eta}{\partial x} = 0 \quad (1)$$

$$fu + g' \frac{\partial \eta}{\partial y} = 0 \quad (2)$$

$$\frac{\partial u}{\partial x} + \frac{\partial v}{\partial y} + \frac{\partial w}{\partial z} = 0 \quad (3)$$

where u, v, w are velocities positive to the east (x), north (y) and upward (z), η the elevation of the interface, $f = \beta y$, $g' \equiv \frac{(\rho_2 - \rho_1)}{\rho_2} g$ where ρ_1 and ρ_2 are the densities of the upper and lower layer respectively and g the gravitational acceleration. The upper layer is assumed to be passive.

For small amplitude disturbances $h + \eta \approx h$, where h is the average height of the layer. By specifying the vertical velocity w_0 as the upwelling velocity through the interface at $z = 0$ and taking u and v independent of z , we obtain after vertical integration of (3)

$$\frac{\partial u}{\partial x} + \frac{\partial v}{\partial y} = -\frac{1}{h} \left(u \frac{\partial h}{\partial x} + v \frac{\partial h}{\partial y} \right) - \frac{w_0}{h} . \quad (4)$$

Cross-differentiating (1) and (2) yields

$$\frac{\partial u}{\partial x} + \frac{\partial v}{\partial y} + \frac{\beta v}{f} = 0 \quad (5)$$

and in the flat interior of the basin where $u \frac{\partial h}{\partial x} = v \frac{\partial h}{\partial y} = 0$ we can now obtain the Sverdrup relation from (4) and (5)

$$v = \frac{w_0 f}{\beta h} . \quad (6)$$

The meridional velocity v is independent of the location of the sinks in the basin. With a positive vertical velocity w_0 it will always be positive and increase with increasing latitude.

From (5) and (6) we get

$$\frac{\partial u}{\partial x} + \frac{2w_0}{h} = 0 \quad (7)$$

from which we obtain the zonal velocity u

$$u = \frac{-2w_0}{h}(x - x_E) \quad (8)$$

where u vanishes at x_E , the eastern boundary.

As there is upwelling in the interior of the basin, there is no constant streamfunction on the lines of constant transport. We can however determine the path of the flow using the definitions

$$u = \frac{dx}{dt} \quad (9)$$

$$v = \frac{dy}{dt} \quad (10)$$

from which we get

$$\frac{u}{v} = \frac{dx}{dy} = -2y(x - x_E) . \quad (11)$$

Integrating from (x_W, y_W) , the point at the foot of the slope from which the trajectory enters the interior, to (x, y) yields the following equation for the trajectory in the interior

$$x = (x_W - x_E) \frac{y_W^2}{y^2} + x_E . \quad (12)$$

Over the slopes where there is no upwelling the streamlines of the flow can be determined by considering conservation of linear potential vorticity (PV)

$$\frac{D}{Dt} \left(\frac{f}{h} \right) = 0 . \quad (13)$$

In a steady state (13) gives

$$u \frac{\partial \left(\frac{f}{h} \right)}{\partial x} + v \frac{\partial \left(\frac{f}{h} \right)}{\partial y} = 0 . \quad (14)$$

With the stream function ψ over the sloping boundaries, we have by definition

$$u = -\frac{\partial \psi}{\partial y} \quad (15)$$

$$v = \frac{\partial \psi}{\partial x} \quad (16)$$

which in (14) yields

$$\frac{\partial \psi}{\partial x} \frac{\partial}{\partial y} \left(\frac{f}{h} \right) - \frac{\partial \psi}{\partial y} \frac{\partial}{\partial x} \left(\frac{f}{h} \right) = J \left(\psi, \frac{f}{h} \right) = 0 \quad (17)$$

where $J(A, B)$ is the Jacobian. From this we deduce that the streamfunction is constant on lines of constant f/h , i.e

$$\psi = \psi_0 \left(\frac{f}{h} \right) \quad (18)$$

where ψ_0 is the value of ψ at the foot of the slope. For the zero order picture we treat the flow as essentially inviscid.

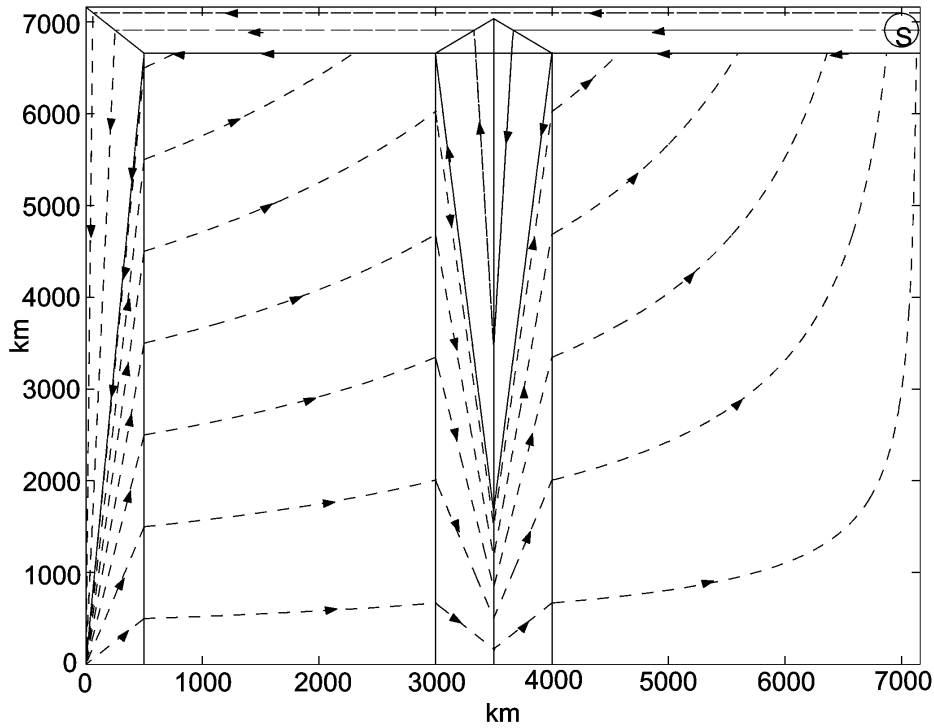


Figure 3: Trajectories of the flow

The resulting flow pattern is shown in Fig. 3. The flow enters the basin in the north-eastern corner. Shallower columns of fluid follow the northern slope on the isobath of entry. Deeper columns encounter the mid-ocean ridge and are diverted southwards and up-slope in order to conserve PV while crossing the eastern side of the ridge. In this nearly inviscid system friction will have to act along the top of the ridge in order to enable flow to cross lines of constant PV. On the western part of the ridge the PV-conserving flow will be northward and down-slope to rejoin the original isobath on the northern slope. The symmetric trajectories are a result of neglecting upwelling over the ridge. Because the

velocities over the narrow ridge are considerably stronger than the velocities induced by upwelling, the trajectory pattern is not significantly different from one which would include upwelling. When reaching the western boundary slope the flow over the north slope will again follow lines of constant PV. In a narrow region at the southwest corner, friction will again be needed to get flow across lines of constant PV so that the fluid can flow northwards to join on to the trajectories of the interior basin where the flow is determined by Sverdrup dynamics.

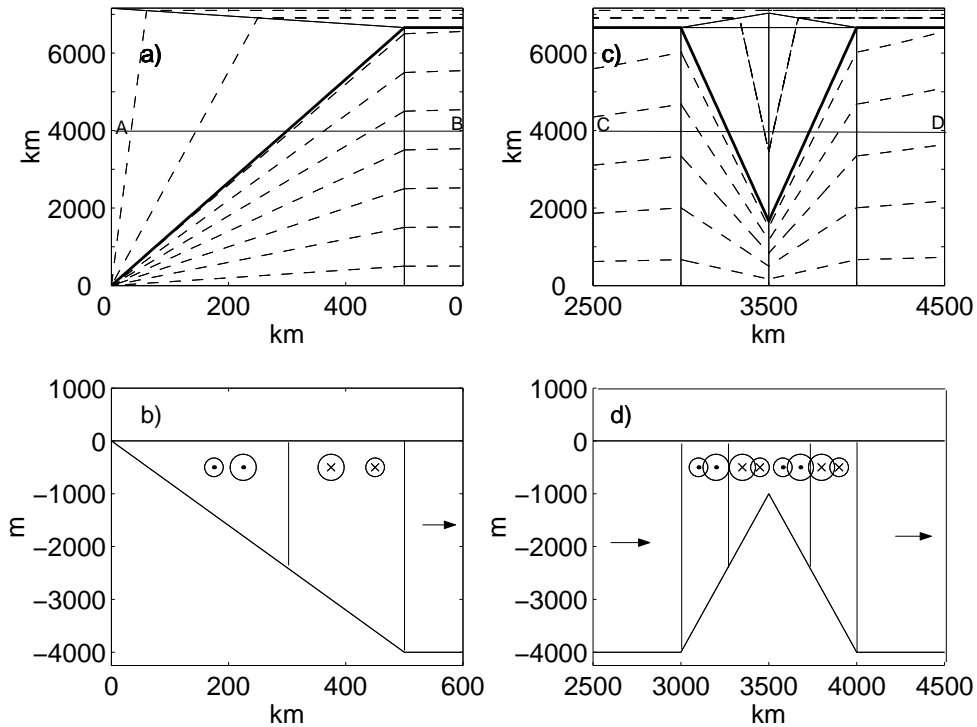


Figure 4: Close-ups and vertical cross-sections of the western boundary and the ridge area. a) The western boundary. b) Section along the line A-B in the western boundary. c) The mid-ocean ridge. d) Section along the line C-D across the ridge.

Fig. 4 shows cross-sections along the lines A-B in the western boundary and C-D across the ridge. The heavy solid line in Fig. 4 a), from (0, 0) to (500, 6660), is the region where all the interior fluid flows southward, coming in to the western boundary layer from the foot of the northern boundary slope. To the west of the heavy line, the transport is also southwards, bringing fluid from the sinking regions. To the east a northward flow supplies the interior with fluid. In the southward flowing region, the transport of fluid will increase eastwards, as shown by the size of the circles in Fig. 4 b), because the transport of sinking water on the northern boundary is proportional to the depth. Hence streamlines originating from a deeper depth contour in the northern boundary will transport more fluid than streamlines from a more shallow depth contour. As the meridional velocity in the interior increases with latitude (Eq. 6), the transport to the eastern side of the solid line decreases eastwards.

As a result of the high speeds on both sides of the intersection between flows in opposing directions, this will be a region of high shear where friction can be expected to be important.

In a similar manner regions of opposing flow at the mid-ocean ridge, as shown by the solid lines in Fig. 4 c) and Fig. 4 d) are regions of high shear. However, we are treating the inviscid limit and friction and diffusion are confined to infinitesimal regions compared to the ocean basin size, and it is assumed that these regions play a rather small part in the overall pattern of the circulation.

The flow pattern at the mid-ocean ridge resembles the picture of Defant's [2] stratospheric circulation in which he used the absolute topography of the 2000-decibar surface to compute the abyssal flow. The result is a Mid Atlantic southward flow, with a northward flow on its eastern side originating from about 5° north, producing a V-shaped mid-ocean flow pattern (corresponding to the dashed lines over the ridge in Fig. 3). Also numerical studies of abyssal flow over topography confirm the pattern seen in Fig. 3. Condie and Kawase [3] used a one and a half layer model to represent the abyssal flow over exponentially sloping side walls at all boundaries and a Gaussian shaped mid-ocean ridge. The eddy activity associated with the sinking region in the north-west corner of the basin in their study has an impact on the flow pattern in the boundary region. The general flow pattern is however confined to closed geostrophic contours, i.e the fluid follows lines of constant f/h and the same V-shaped structure of the flow is visible at the mid-ocean ridge.

3 The two-layer model

In section 2, a geometrical picture was obtained on how the influence of sloping topography will alter the boundary layer flow of a homogeneous fluid. Extending the theory to a baroclinic flow, we will study the simplest case, two layers of inviscid fluid with uniform densities ρ_1 and ρ_2 . The flat bottom interior solution to a two-layered model of the abyssal flow on a spherical earth was studied by Veronis [4]. The outline of that paper is followed, but here with a β -plane approximation. The steady state of each layer in the interior is geostrophic, hydrostatic and described by the vertically integrated equations

$$fV_1 = gh \frac{\partial h_1}{\partial x} \quad (19)$$

$$fU_1 = -gh \frac{\partial h_1}{\partial y} \quad (20)$$

$$\frac{\partial U_1}{\partial x} + \frac{\partial V_1}{\partial y} = w_0 \quad (21)$$

$$fV_2 = gh_2 \frac{\partial}{\partial x} \left(\frac{\rho_1}{\rho_2} h_1 + \frac{\Delta\rho}{\rho_2} \right) \quad (22)$$

$$fU_2 = -gh_2 \frac{\partial}{\partial y} \left(\frac{\rho_1}{\rho_2} h_1 + \frac{\Delta\rho}{\rho_2} h_2 \right) \quad (23)$$

$$\frac{\partial U_2}{\partial x} + \frac{\partial V_2}{\partial y} = -\frac{\rho_1}{\rho_2} w_0 . \quad (24)$$

Here U and V are the vertically integrated zonal and meridional velocities, h the thick-

ness of the upper layer and h_1 and h_2 the heights of the upper surface and interface respectively so that

$$h_1 = h + h_2 . \quad (25)$$

Cross-differentiating the momentum equations and making use of the continuity equations for each layer gives the relations

$$\beta V_1 = -fw_0 - gJ(h, h_1) \quad (26)$$

$$\beta V_2 = \frac{\rho_1}{\rho_2} (fw_0 + gJ(h, h_1)) . \quad (27)$$

From (26) and (27) we find that the total mass transport is equal and opposite at each point, i.e.,

$$\frac{\rho_1}{\rho_2} V_1 + V_2 = 0 . \quad (28)$$

Taking the sum of $\rho_1/\rho_2 \times (19)$ and (22) we now have

$$\frac{\rho_1}{\rho_2} V_1 + V_2 = \frac{g}{2f} \frac{\partial}{\partial x} \left(\frac{\rho_1}{\rho_2} h_1^2 + \frac{\Delta\rho}{\rho_2} h_2^2 \right) = 0 . \quad (29)$$

From (29) we can obtain an expression for the variation of the upper layer height h_1 in the x -direction:

$$\frac{\rho_1}{\rho_2} h_1 \frac{\partial h_1}{\partial x} = -\frac{\Delta\rho}{\rho_2} h_2 \frac{\partial h_2}{\partial x} = -\frac{\Delta\rho}{\rho_2} (h_1 - h) \frac{\partial}{\partial x} (h_1 - h) . \quad (30)$$

Replacing h_1 with H , the mean basin depth, where h_1 appears as a coefficient and neglecting the term $\frac{\Delta\rho}{\rho_2} \frac{h}{H} \frac{\partial h_1}{\partial x}$ we have

$$\frac{\partial h_1}{\partial x} = \frac{\Delta\rho}{\rho_2} \left(1 - \frac{h}{H} \right) \frac{\partial h}{\partial x} . \quad (31)$$

Integrating (31) gives

$$h_1 = h_{1E} + \frac{\Delta\rho}{\rho_2} \left(h - \frac{h^2}{2H} - \left(h_E - \frac{h_E^2}{2H} \right) \right) \quad (32)$$

from which, with a constant h_{1E} and h_E at the eastern wall, we obtain

$$\frac{\partial h_1}{\partial y} = \frac{\Delta\rho}{\rho_2} \left(1 - \frac{h}{H} \right) \frac{\partial h}{\partial y} . \quad (33)$$

From (31) and (33) we see that $J(h, h_1) = 0$, so from (26) and (27) we can now obtain the vertically averaged meridional velocities in the upper and lower layer

$$V_1 = -\frac{fw_0}{\beta} \quad (34)$$

$$V_2 = \frac{\rho_1}{\rho_2} \frac{fw_0}{\beta} . \quad (35)$$

The zonal velocities can be derived using (34) and (35) in (21) and (24) respectively, which gives

$$U_1 = 2w_0(x - x_E) \quad (36)$$

$$U_2 = -\frac{\rho_1}{\rho_2} 2w_0(x - x_E) . \quad (37)$$

Using (31) in (19) yields

$$fV_1 = g' \frac{\partial}{\partial x} \left(\frac{h^2}{2} - \frac{h^3}{3H} \right) \quad (38)$$

and using (34) for V_1 , this can now be integrated from x to x_E and we can specify h by

$$\frac{h^2}{2} - \frac{h^3}{3H} = \frac{h_E^2}{2} - \frac{h_E^3}{3H} + \frac{f^2 w_0}{g' \beta} (x_E - x) . \quad (39)$$

As in the homogeneous case we can now get the trajectories of the flow from the zonal and meridional velocities.

Considering zonally integrated transport balances for the system, we have that the interior transport in the upper layer, T_1 , across a zonal line y is given by integrating V_1 over the basin width. With T_1 taken positive northwards we get

$$T_1 = -w_0(x_E - x_W)y . \quad (40)$$

The upper layer gains water from the total upwelling, W , taking place north of y . This is given by integrating w_0 over the width and length of the basin

$$W = w_0(x_E - x_W)(y_N - y) . \quad (41)$$

As the sinking takes place in the northeastern corner, there is a net loss of upper layer fluid of amount S to the lower layer and

$$S = -w_0(x_E - x_W)y_N . \quad (42)$$

To obtain a mass balance for the basin, the transport T_W carried in the western boundary current is

$$T_W = S - W - T_1 = 2w_0(x_E - x_W)y . \quad (43)$$

From (43) it can be seen that across each zonal line, the western boundary current must carry twice the interior transport.

Having obtained a solution for the flat bottom interior, we will now seek a solution for a two-layer system with bottom topography. Salmon [5] considered the planetary geostrophic equations for a two-layer system over a sloping western boundary. In his notation the governing equations for a frictionless steady state read

$$\mathbf{f} \times \mathbf{u}_1 = -\nabla\phi_s \quad (44)$$

$$\mathbf{f} \times \mathbf{u}_2 = -\nabla\phi_s + g'\nabla h \quad (45)$$

$$\nabla \cdot (\mathbf{u}_i h_i) = 0, \quad i = 1, 2 \quad (46)$$

where $\mathbf{u}_i \equiv (u_i, v_i)$ are the horizontal velocities and ϕ_s is the pressure at the surface divided by a reference density.

Adding (46) for $i = 1$ and $i = 2$ yields

$$\nabla \cdot (h_1 \mathbf{u}_1 + h_2 \mathbf{u}_2) = 0 \quad (47)$$

and thus

$$h_1 \mathbf{u}_1 + h_2 \mathbf{u}_2 = \mathbf{k} \times \nabla \Psi \quad (48)$$

where \mathbf{k} is the vertical unit vector and Ψ the total transport streamfunction. Eq. (44) and (45) gives

$$\mathbf{f} \times (\mathbf{u}_1 - \mathbf{u}_2) = -g'\nabla h . \quad (49)$$

From (48) and (49)

$$\mathbf{u}_1 = \frac{1}{H} \mathbf{k} \times \nabla \Psi + \frac{g'h_2}{fH} \mathbf{k} \times \nabla h \quad (50)$$

$$\mathbf{u}_2 = \frac{1}{H} \mathbf{k} \times \nabla \Psi - \frac{g'h_1}{fH} \mathbf{k} \times \nabla h \quad (51)$$

and using (50) and (51) and taking the curl of the vertical average of (44) and (45) we can write the total streamfunction equation as

$$J\left(\frac{f}{H}, \Psi\right) + J\left(\frac{1}{2}g'h^2, \frac{1}{H}\right) = 0 . \quad (52)$$

From (46) and (50) we get an equation for the upper layer thickness

$$J\left(\Psi, \frac{h}{H}\right) + J\left(g'h, \frac{h}{f}\left(1 - \frac{h}{H}\right)\right) = 0 . \quad (53)$$

By defining

$$q_1 \equiv \frac{h}{f}, \quad q_2 \equiv \frac{H-h}{f} \quad (54)$$

it can be shown that (52) and (53) can be written in the forms

$$J(\Psi, q_1) + q_2 J(g'h, q_1) = 0 \quad (55)$$

$$J(\Psi, q_2) - q_1 J(g'h, q_2) = 0 \quad (56)$$

which describes the PV in the upper and lower layers.

Salmon [5] obtained general solutions to (55) and (56) for the two cases $J(q_1, q_2) \neq 0$ and $J(q_1, q_2) = 0$. In the latter case he showed that a solution is possible only if either q_1 or q_2 is constant in a particular region. That would appear to be simply a mathematical curiosity but he showed, in fact, that one can obtain realistic features in the vicinity of the Gulf Stream by making use of $q_1 = \text{constant}$ and $q_2 = \text{constant}$ in different regions near the Gulf Stream.

We have sought a solution with $q_1 = \text{constant}$ in the slope regions. In order for that to be a valid solution it is necessary that it match to the interior solution at the foot of the slope in the different regions. The latter comes from (39). In the special case with $h_E = 0$, we can obtain a solution with constant q_1 if we take the lowest order solution to (39) by neglecting the term with H in the denominator (neglecting that term involves a maximum error of about 5 % but a correction for that term can be taken into account iteratively). The resulting solution is

$$h^2 = \frac{2f^2 w_0}{g' \beta} (x_E - x) . \quad (57)$$

Evaluating (57) at the western edge of the interior, i.e. $x = x_W \approx 0$, we have

$$\frac{h}{f} = \left(\frac{2w_0}{g' \beta} x_E \right)^{\frac{1}{2}} . \quad (58)$$

So $h/f = \text{constant}$ is an exact solution over the western boundary slope and it also matches the interior at the eastern edge of the boundary. Therefore, h is constant on lines of constant y in the boundary layer and is given by the thickness of the interior upper layer at $x = x_W$.

From the planetary geostrophic equation for the lower layer, (45), we also have

$$\frac{f}{h_2} (\mathbf{u}_2 h_2) = \mathbf{k} \times (\nabla \phi_s - g' \nabla h) . \quad (59)$$

As we neglect the upwelling in the boundary layer, we have $\nabla \cdot (\mathbf{u}_2 h_2) = 0$ so the divergence of (59) yields

$$\mathbf{u}_2 h_2 \cdot \nabla \frac{f}{h_2} = 0 \quad (60)$$

and with $\mathbf{u}_2 h_2 = \mathbf{k} \times \nabla \psi_2$ we have

$$J \left(\psi_2, \frac{f}{h_2} \right) = 0 . \quad (61)$$

With h constant on lines of constant y , h_2 can be determined from $h_2 = H - h$ and with ψ_2 constant on lines of constant $\frac{h_2}{f}$ in the boundary layer, we can match the upper and lower

layer solutions to the interior solutions at the foot of the slope. With the same reasoning for the mid-ocean ridge area we get the lower layer flow pattern shown in Fig. 5. The dashed lines are the trajectories of the flow and the solid lines in the interior are contours of the lower layer height h_2 . The upper layer thickness is set to zero at the eastern boundary and the mean basin depth is 4000 m. The upwelling velocity is specified to $2 \cdot 10^{-7}$ m/s and $\Delta\rho/\rho_2 = 0.0015$.

Given that $\frac{h}{f} = \text{constant}$ over the mid-ocean ridge, when crossing the ridge, the lower layer flow follows lines of constant $\frac{h_2}{f}$. The path is again symmetric about the center of the ridge.

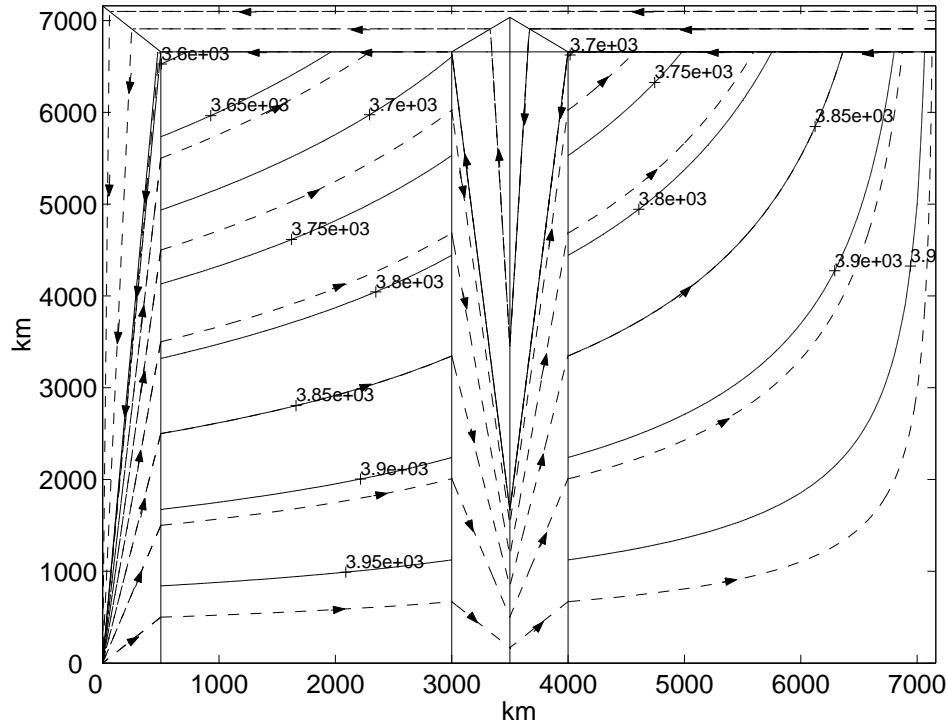


Figure 5: Flow pattern of the lower layer. The calculations were made for $w_0 = 2 \cdot 10^{-7}$ m/s, $h_E = 0$ m and $\Delta\rho/\rho_2 = 0.0015$

The westward jet along the foot of the northern slope turns southward at the northwest corner of the interior and continues as a jet toward the southwest corner. To the west of that jet, water that has sunk in the north will move southwards on lines of constant $\frac{h_2}{f}$ set by the lower layer depth on the northern boundary. On the eastern side of the $\frac{h_2}{f}$ line carrying the interior water southward, fluid flows northward along lines of constant $\frac{h_2}{f}$ to the interior. The vicinity of the region separating southward and northward flow must represent a region of intense shear. Therefore, friction is likely to be important here.

The upper layer flow pattern is shown in Fig. 6. In the interior the trajectories are the same as for the lower layer but in the opposite direction so the fluid moves in a south-

westward direction. Contours of upper layer thickness are parallel to the paths of the trajectories. Over the western boundary slope and over the mid-ocean ridge, the upper layer flow is zonal on lines of constant $\frac{h}{f}$.

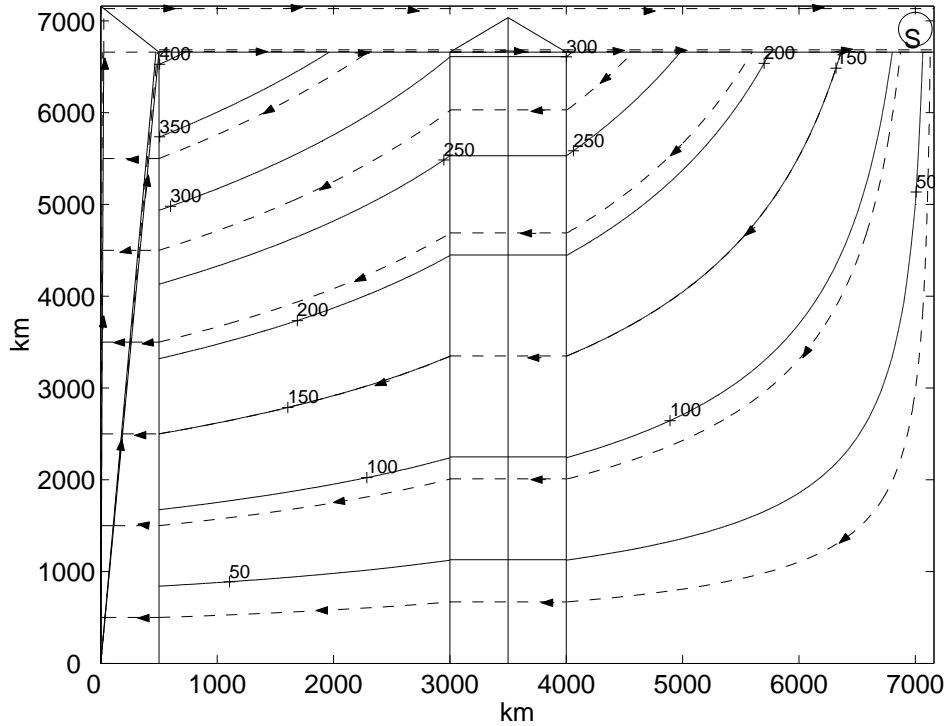


Figure 6: Flow pattern of the upper layer

Just south of the southern edge of the northern boundary, the upper layer western boundary transport is, due to conservation of mass

$$T_W = S + T_I . \quad (62)$$

Just north of that edge, the interior transport is zero, which gives

$$T_W = S . \quad (63)$$

Hence, there must be a jet that heads eastward along the foot of the slope from the northwestern corner of the interior. Just as the lower layer takes fluid from the westward jet along the foot of the north slope and transports it southward along the line of constant $\frac{h_2}{f}$ that goes from the northwestern corner of the interior to the southwestern corner on the western slope, the upper layer must deliver an equal amount of fluid northeastward to supply the eastward flow along the southern edge of the northern slope. So there will be a jet in the western boundary upper layer flow, also along this line of constant $\frac{h_2}{f}$. In that jet, to induce the northward transport in the upper layer, the sea surface will rise sharply toward the east. We must also have a compensating drop of the interface. The displacement

of the interface across the western boundary jet can be obtained from the equations for the upper and lower layer

$$\rho_1 f V_1 = \rho_1 g h \frac{\partial \eta_1}{\partial x} \quad (64)$$

$$\rho_2 f V_2 = g h_2 \frac{\partial}{\partial x} (\rho_1 \eta_1 + \Delta \rho \eta_2) \quad (65)$$

where subscript 1 and 2 denotes the upper and lower layer respectively. As the transports in the upper and lower layer are equal and opposite, Eq.(28) is valid also in the jet, i.e. the total transport vanishes at each point in the jet. From (64) and (65) we then get

$$\frac{\partial \eta_2}{\partial x} = - \frac{\rho_1 H}{\Delta \rho h_2} \frac{\partial \eta_1}{\partial x} . \quad (66)$$

As $h = \eta_1 + \bar{h} - \eta_2$, where \bar{h} is the mean upper layer depth, we have that

$$\frac{\partial \eta_2}{\partial x} = \frac{\partial \eta_1}{\partial x} - \frac{\partial h}{\partial x} . \quad (67)$$

Applying (67) to (66) we find that

$$\frac{\partial \eta_1}{\partial x} \approx \frac{\Delta \rho h_2}{\rho_1 H} \frac{\partial h}{\partial x} \quad (68)$$

and (64) becomes

$$f V_1 = \frac{g \Delta \rho h_2}{2 \rho_1 H} \frac{\partial h^2}{\partial x} . \quad (69)$$

Since the assumption is of an infinitesimally thin jet, we can consider h_2/H to be constant. Eq. (69) can then be integrated in the x-direction and becomes

$$f T_1 = \frac{g \Delta \rho h_2}{2 \rho_1 H} (h_R^2 - h_L^2) \quad (70)$$

where subscript R and L denotes the right and left edge of the jet respectively.

As the upper layer thickness on the right edge of the jet is equal to the upper layer depth at the western boundary of the interior, we obtain the equation for the upper layer thickness at the western side of the jet

$$h_L^2 = h_W^2 - \frac{2 f T_1}{g} \frac{\rho_1}{\Delta \rho} \frac{H}{h_2} . \quad (71)$$

On the western side of the jet, the upper layer thickness is again constant and the transport is again purely zonal. Close to the western edge of the boundary layer, there will be a triangular wedge of only upper layer water, also with northward transport as the streamfunction must go to zero at the western edge of the boundary layer. So of the northward transport of upper layer water, the portion contributed by the jet feeds the northern boundary layer that supplies water to the interior and the portion contributed by the boundary current near the western edge of the basin supplies an equal amount of water to the sink.

A schematic of cross-sections of the western boundary, the ridge area and the northern boundary is shown in Fig. 7.

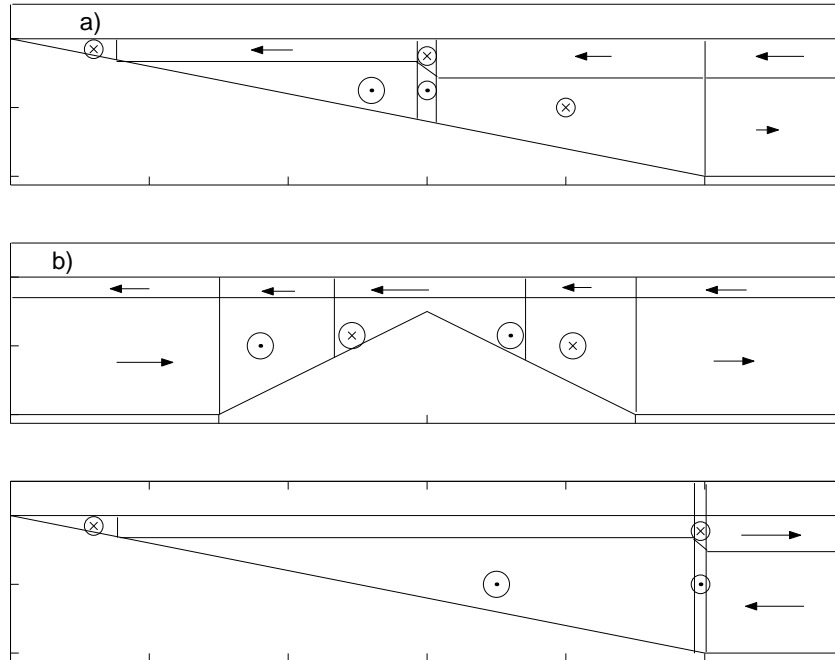


Figure 7: Schematic of zonal cross-sections of a) western boundary b) mid-ocean ridge area and c) meridional cross-section (looking eastward) of the northern boundary

In Fig. 7 a), the westward transport in the constant upper layer carries water to the northward jet. The upper layer thickness decreases across the jet and on the other side of the jet the upper layer thickness is again constant and carries water westward to the northward boundary current. In the lower layer, the region closest to the western edge of the boundary layer carries the sinking water southwards from the northern boundary. The southward moving jet in the lower layer carries water from the interior. On the eastern side of the jet, a northward flow supplies the interior with fluid.

Over the mid-ocean ridge (Fig. 7 b)) the upper layer thickness is constant and the flow purely westwards. In the lower layer, the inner region of the ridge is where the sinking water flows southward and then northward to cross the ridge. In the two outer regions of the ridge, fluid from the interior crosses the ridge. Along the lines joining the two regions the shear is intense and friction must be important.

On the northern slope (Fig. 7 c) the upper layer jet at the southern edge of the boundary supplies fluid to the interior while the current at the northern edge of the boundary layer provides water to the sink. The transport of water to the sinking regions must spread out across the upper layer, but the details of this flow have not been further considered. In the lower layer jet, water from the interior is carried westward and north of the jet the water that has sunk is carried to the western boundary layer.

4 Discussion

It has been shown that the presence of sloping boundaries considerably affects the flow pattern. In the presence of a mid-ocean ridge, dividing the ocean in two halves, the flow is diverted considerably to the south in order to continue to the other basin.

In the homogeneous case the flow will follow lines of constant f/h in order to conserve potential energy. The same holds when the fluid crosses the mid-ocean ridge and has to turn southward in order to decrease the depth of the water column.

In the two-layer model we have shown a simple solution consistent with an exact solution to the general equations (55) and (56) for the case when $J(q_1, q_2) = 0$. The solution keeps the upper layer thickness constant on lines of constant y in the western boundary layer and the ridge area. In the lower layer the transport streamfunction follows lines of constant $\frac{h_2}{f}$. The solution requires a northward jet in the upper layer of the western boundary layer and the jet will continue eastward along the foot of the north slope. Although friction must be clearly be important in parts of the slopes, we have confined the analysis to the inviscid limit using transport balance arguments. This led to the conclusion that half of the total northward transport in the western boundary layer will take place in the jet and half of the transport will occur in a triangular wedge occupied by only upper layer water along the western edge of the western slope. As the streamfunction must be zero at the western edge, the transport will have to turn northwards and the dynamics will be that of a single layer fluid. The exact dynamics of the northern boundary have not been analyzed, but the flow will more or less follow lines of constant H (total depth) in this region as $y \sim \text{constant}$ and $H - h \sim H$ except close to the northern edge where we again have dynamics of a single layer as the total depth goes to zero. Upper layer water sinks in the northeastern corner and flows westward in the lower layer of the northern boundary region and then southward along lines of constant f/h_2 to the southwest corner of the western boundary slope. The exact path can not be determined here, due to the absence of a complete picture of the northern boundary upper layer thickness.

The reasoning holds for slope regions that are very narrow compared to the basin size. The analytical solution was pieced together, treating the slope regions in the inviscid limits. As it turned out, friction must be important in isolated regions over the slopes. It allows the fluid to cross lines of constant PV where needed and it will also be required to smooth out the abrupt change in direction of flow over the slopes. A numerical model of this system should help to determine how much of this study is consistent with the full equations including friction. A next step analytically would be to try to include wind stress in addition to the upwelling.

5 Acknowledgments

I wish to express my sincere thanks to George Veronis, for the uncountable hours of discussion, his friendship and for the nice walks. The fellows provided many laughs and kept me sane during the last weeks of hectic work. Everyone that passed through Woods Hole and Walsh Cottage made the summer of 2001 a very memorable one.

References

- [1] H. M. Stommel, "The abyssal circulation," *Deep-Sea Res.* **5**, 80 (1958).
- [2] A. Defant, *Die absolute topographie des phys. meeresniveaus und der druckflächen, so wie die wasswer bewegungen im Atl. Ocean* (Meteor Werk. 6/2, 5, Lief. Berlin, 1941).
- [3] S. A. Condie and M. Kawase, "Models of abyssal flow in basins separated by a mic-ocen ridge," *J. Mar. Res.* **50**, 199 (1992).
- [4] G. Veronis, "Model of world ocean circulation: II. Thermally driven, two-layer," *J. Mar. Res.* **34**, 421 (1976).
- [5] R. Salmon, "A two-layer Gulf Stream over a continental slope," *J. Mar. Res.* **50**, 341 (1992).